

## Direct radiative properties of modern European woodstove emissions: effect of photochemical aging and an electrostatic precipitator

A. Mukherjee<sup>1</sup>, A. Paul<sup>2</sup>, M. Ihalainen<sup>1</sup>, M. Somero<sup>1</sup>, S. Basnet<sup>1</sup>, A. Virkkula<sup>3</sup>, R. Zimmermann<sup>4\*</sup>, O. Sippula<sup>1\*</sup>

<sup>1</sup>Department of Environmental and Biological Sciences, University of Eastern Finland, Kuopio, 70211, Finland, <sup>2</sup>Department of chemistry, Aarhus university, 8000 Aarhus, Denmark, <sup>3</sup>Atmospheric Composition Research, Finnish Meteorological Institute, 00101, Helsinki, Finland, <sup>4</sup>Chair of Analytical Chemistry, University of Rostock, Rostock, 18059, Germany

Residential wood combustion (RWC) is a major source of carbonaceous aerosols in Europe, yet large uncertainties remain in assessing the climate impacts of emissions from modern wood stoves. We investigated the physical, chemical, and optical properties of aerosols emitted from combustion of beech woodlogs in an air-staged chimney stove. Each experiment lasted for 4 hours and consisted of the burning of 6 batches of logwood. Fresh emissions were characterized with and without an electrostatic precipitator (ESP, Oekotube). In addition, emitted aerosols were photochemically aged using an oxidation flow reactor (PEAR) under two different OH exposures corresponding to equivalent aging upto ~1.4 (short aging) and ~3 (medium aging) atmospheric days.

Emissions of CO<sub>2</sub>, CO and major non-methane VOCs were monitored using an online Fourier-Transform Infra-Red spectrophotometer (FTIR). The temporal evolution of CO<sub>2</sub> and CO was used to calculate time series of modified combustion efficiency, as well as to define distinct combustion phases, namely ignition, flaming and residual char burning [1]. Light absorption ( $\beta_{\text{abs}}$ ) and scattering coefficients ( $\beta_{\text{sca}}$ ) of fresh and aged aerosols were measured using a multi-wavelength aethalometer (AE33) and integrating nephelometer, respectively. Equivalent black carbon (eBC) concentration and fraction of total light absorption by brown carbon (BrC) were also estimated from AE33. Chemical composition of organic (OA) and inorganic aerosol were estimated by an aerosol mass spectrometer. Timeseries of aerosol particle size distributions were measured by a scanning mobility particle sizer (SMPS), as well as an electrical low-pressure impactor (ELPI). Finally, Simple forcing efficiency (SFE, W g<sup>-1</sup>) of fresh and aged aerosols over both average global terrain and fresh snow surface were estimated as per previous literature [2] using albedo values of 0.19 and 0.8 respectively.

Fresh emissions were dominated by soot-rich particles with low single scattering albedo (SSA) and high mass absorption coefficients (MAC), particularly during flaming combustion phases. We also observed presence of dark BrC (or strongly absorptive BrC) in emissions from flaming combustions. The ESP reduced overall OA and eBC emissions respectively by approximately 80% and 69%, but altered particle size distributions and increased mean volume diameter (VMD) of fresh emissions due to size and particle composition dependent collection efficiency. As a result, fresh RWC emission was more soot-rich yet relatively more scattering (with 44% higher SSA<sub>550</sub>) in presence of ESP. Photochemical aging led to substantial secondary organic aerosol (SOA) formation, increasing OA/eBC ratios as well as VMD, due to condensation of SOA. As a result, we observed enhanced  $\beta_{\text{sca}}$  and reduced  $\beta_{\text{abs}}$  in aged emissions compared to fresh emissions. Consequently, short and medium aging decreased SFE estimated over average global terrain by 39% and 43% respectively, compared to that of fresh RWC emission (96.3±88.3 W g<sup>-1</sup>). However, estimated SFE values were still positive even after aging, suggesting significant warming potential of RWC emitted particles from modern woodstoves.

[1] Mukherjee, A., et al., *Science of the Total Environment*, 2024, 952, 175840.

[2] Chen, Y. and Bond, T.C., *Atmospheric Chemistry and Physics*, 2010, 10(4), 1773-1787

## Spatiotemporal modelling of ambient concentration of ultrafine particles in Switzerland

E. P. Twomey<sup>1,2</sup>, J. Keller<sup>1,2</sup>, S. Loup<sup>1,2</sup>, M. Grünig<sup>1,2</sup>, M. Dijk<sup>3</sup>, J. Kerckhoffs<sup>3</sup>, K. de Hoogh<sup>3</sup>, M. Rössli<sup>1,2\*</sup>, M. Eeftens<sup>1,2\*</sup>

<sup>1</sup>University of Basel, Faculty of Science - Epidemiology, Basel, Basel-Stadt, Switzerland, <sup>2</sup>Swiss Tropical and Public Health Institute, Environmental Epidemiology, Allschwil, Basel-Land, Switzerland, <sup>3</sup>Division of Environmental Epidemiology, Institute for Risk Assessment Sciences, Utrecht University, Utrecht, the Netherlands

**Keywords:** Ultrafine particles, air pollution, spatiotemporal modelling, particle number concentration, random forest

### Introduction

Despite mechanistic evidence from toxicological studies, large-scale epidemiological evidence for health effects of ultrafine particles (UFP) remains limited due to sparse monitoring. UFP exhibit large spatial and temporal contrasts, and while several spatial models have been published, few so far incorporate temporal variability. Within the framework of the MARKOPOLO (“Markers of Pollution”) project, we aimed to develop a national, three-season, high-resolution (daily, 25x25m) spatiotemporal model which can be harnessed to estimate exposure for cohorts across Switzerland.

### Methods

The project is conducting UFP measurements in Switzerland with national coverage between June 2025 and April 2026 using a mobile platform, visiting all major cities, many smaller towns and a selection of minor villages, balancing population coverage and capturing the full range of concentration contrasts. Ultrafine particle number concentration (PNC) was measured using an EPC 3787 at 1-second intervals, alongside co-pollutants (PM<sub>2.5</sub>, NO<sub>x</sub>, black carbon), GPS position, temperature and relative humidity. Random forest models were developed to predict logged PNC using spatial and temporal environmental predictors such as altitude, meteorology, land-use and road type data.

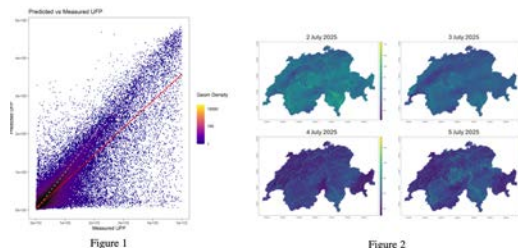


**Figure 1:** Measured versus predicted UFP number concentration. The dashed line indicates the 1:1 ratio. The red line indicates a slight typical underestimation of the model as compared to measured concentrations. This is due to scatter on the lower right end of the graph, which results from high-exposure outliers on roads. These are challenging to predict due to highly specific local or temporary emissions or conditions, which are not captured by any of the predictors.

**Figure 2:** Swiss-wide prediction of UFP number concentration across Switzerland on 4 consecutive days in July 2025. Concentrations are shown as the log(ultrafine particle number concentration [#particles/cm<sup>3</sup>]). Predicted concentrations range roughly between  $e8 \approx 2980$  particles/m<sup>3</sup> and  $e12 \approx 163000$  particles/m<sup>3</sup>.

### Results

During the summer measurement period (16 June – 4 August 2025), 50 days and 5115km of data captured on Swiss roads yielded a median level of 7700 particles/m<sup>3</sup> [interquartile range 5800-8500 particles/m<sup>3</sup>]. We measured within 100m of the homes of 4.5% of the Swiss population. The performance of our preliminary Swisswide model yielded an overall R<sup>2</sup> of 0.90 (Figure 1). Road length of motorways and traffic intensity in buffers of 100-500m and weather-related variables (temperature, humidity) were the most important predictors. Example predictions for four consecutive summer days are shown in Figure 2.

### Conclusion

We provide some of the first spatiotemporal national concentration models for ultrafine PNC, allowing timevarying exposure assessment for health studies.

## How coating pathway controls light absorption by black carbon

C. Jourdain<sup>1,2</sup>, J. Symonds<sup>3</sup>, Z. Sun<sup>4</sup>, M. Gysel Beer<sup>4</sup>, A. Boies<sup>1,2</sup>

<sup>1</sup>Mechanical Engineering Department, Stanford University, 452 Escondido Mall, 94305, Stanford, USA, <sup>2</sup>Department of Engineering, University of Cambridge, Trumpington St, Cambridge CB2 1PZ, UK, <sup>3</sup>Cambustion Ltd, 347 Cherry Hinton Road, Cambridge, CB1 8DH, UK, <sup>4</sup>PSI Center for Energy and Environmental Sciences, 5232 Villigen PSI, Switzerland

Black carbon (BC) aerosols are among the most important climate-forcing agents in the Earth's atmosphere, yet the interaction of light with individual BC cores and their coating remains actively debated [1]. After emission, BC particles rapidly mix with non- or weakly-absorbing material through condensation and coagulation, altering their morphology, radiative properties, and atmospheric lifetime [2]. However, the impact of these distinct coating pathways is difficult to disentangle in ambient observations.

Here, we independently investigate condensation- and coagulation-driven coating mechanisms using controlled laboratory experiments combined with numerical optical modeling. Two custom-built aerosol chambers are used to generate mixed BC particles by coating soot with an atmospheric liquid surrogate via either evaporation–condensation or coagulation with oppositely charged droplets. The resulting particles are characterized in real time in terms of size, mass, and wavelength-dependent optical absorption. In parallel, single-particle optical properties are simulated using the discrete dipole approximation and multi-sphere T-matrix methods.

We find that the coating pathway governs particle morphology and, consequently, optical absorption. Condensation leads to encapsulated, near-spherical BC particles, whereas coagulation produces irregularly-shaped aggregates. The mass absorption cross-section (MAC) of condensed BC increases systematically with coating mass at 405, 532, and 781 nm, with stronger enhancement at shorter wavelengths (e.g.,  $\text{MAC}_{405 \text{ nm}} = 13.9 \text{ m}^2\text{g}^{-1}$  at a mass ratio of 4). In contrast, the MAC of coagulated BC remains largely insensitive to coating amount and only slightly exceeds that of fresh BC (e.g.,  $\text{MAC}_{405 \text{ nm}} = 12.1 \text{ m}^2\text{g}^{-1}$  at a mass ratio of 4). Consequently, even lightly condensed BC exhibits higher absorption than coagulated BC, a trend consistently reproduced in optical simulations.

These results demonstrate that coating morphology, rather than coating mass alone, controls BC absorption enhancement. Accounting for coating-dependent shape and mixing state can help reconcile discrepancies in field-derived absorption enhancements and reduce uncertainties in BC representation in regional and global climate models.

[1] C. D. Cappa *et al.*, *Science*, 2012, 337, 1078-1081.

[2] T. C. Bond, R. W. Bergstrom, *Aerosol Science and Technology*, 2006, 1, 27–67.

## Transient formation of organic gaseous emissions in residential wood combustion with and without an electrostatic precipitator

A. Hartikainen<sup>1</sup>, A. Mukherjee<sup>1</sup>, M. Somero<sup>1</sup>, Z. Fang<sup>2</sup>, Y. Rudich<sup>2</sup>, R. Zimmermann<sup>3,4</sup>, O. Sippula<sup>1,5\*</sup>

<sup>1</sup>Dept. of Environmental and Biological Sciences, University of Eastern Finland, FI-70211, Kuopio, Finland, <sup>2</sup>Dept. of Earth and Planetary Science, Weizmann Institute of Science, 7610001 Rehovot, Israel, <sup>3</sup>Analytical Chemistry, University of Rostock, D-18059 Rostock, Germany, <sup>4</sup>Helmholtz Zentrum München, D-85764 Neuherberg, Germany, <sup>5</sup>Dept. of Chemistry, University of Eastern Finland, FI-80101 Joensuu, Finland

Residential wood combustion can be a major source of atmospheric organic aerosols emitted in both gaseous and particle phases. In this work, we aimed to resolve the temporal behavior of the gaseous organic emissions and determine the impacts of an electrostatic precipitator (ESP) on their release. Batches of beech logs were combusted in an air-staged chimney stove (6 batches per 4 h experiment). For half of the experiments, an OekoTube (Oekosolve) 'electrostatic precipitator inside' -unit was installed in the flue gas stack (n=4 with ESP off, n=4 with ESP on). Volatile organics were monitored by a proton transfer reactor - time of flight - mass spectrometer (PTR-ToF 8000, Ionicon) alongside extensive particle phase measurements.

The organic gaseous emissions were at their highest during batch ignition. As the combustion progressed to flaming conditions and the combustion temperature increased, organic gases were effectively oxidized in the flame, leading to pyrosynthesis of the organics and increase in the particulate emissions [1]. Slower ignition in the cold stove during the first batch led to a distinctly different emission profile compared to the later batches. The total organic gaseous emissions increased again for the later (fourth to sixth) batches, likely due to the faster combustion rate driven by the increased temperature.

Five distinct factors were resolved from the mass spectra time series by non-negative matrix factorization (NMF). Ignition phases were linked to two factors: one prominent for the cold ignition of first batch (dominated by acetic acid), one for the high temperature ignition of later batches (dominated by benzene). A factor comprised dominantly of nitromethane was linked with the flaming phase and correlated best with the particulate brown carbon emissions. The fourth factor may be linked to direct cellulose depolymerization products, as it contained the furan emissions. The fifth factor contained both polycyclic aromatic hydrocarbons (PAHs) and oxidized aromatics. In contrast to the other factors, its concentration grew towards the end of each batch.

The overall emission profile was similar with or without the ESP. However, the emission factors of PAHs and oxygenated polycyclic compounds (o-PAHs) were statistically significantly higher with the ESP on for all the combustion phases, with batchwise enhancement ratios of 1.8 and 1.5 for PAHs and o-PAHs, respectively. The increase was most prominent towards the end of combustion ('ember phase'), when the ESP reduced particulate emissions especially efficiently [1], and likely caused by the decreased adsorption of polycyclic compounds onto particle phase when particle emissions were reduced.

[1] Mukherjee A. et al., *Science of the Total Environment*, **2024**, 952, 175840

## Dynamics of urban particle number size distributions in Stockholm, Sweden

D. Schlesinger<sup>1,2</sup>, S. Silvergren<sup>1</sup>, M. Norman<sup>1</sup>, Ö. Axelsson<sup>3,4</sup>, S. L. Haslett<sup>2\*</sup>

<sup>1</sup>SLB-analys, Environment and Health Administration, City of Stockholm, Sweden, <sup>2</sup>Department of Environmental Science, Stockholm University, Stockholm, Sweden, <sup>3</sup>Centre for Occupational and Environmental Medicine, Region Stockholm, Stockholm, Sweden, <sup>4</sup>Institute of Environmental Medicine, Karolinska Institute, Stockholm, Sweden

Air pollution has a strong impact on human health [1]. Although growing scientific evidence shows that the smallest particles — so-called ultrafine particles (UFP)—are especially harmful to human health, it is mainly the coarse particle fractions (PM<sub>10</sub> and PM<sub>2.5</sub>) that are regularly measured against standards and reported in cities worldwide. As a consequence, data about UFP in urban environments is still very limited.

The Environment and Health Administration of the City of Stockholm has measured UFP in the urban background and in street canyons since 2002, and the time-series of particle number concentration (PNC) for Stockholm can now be considered one of the longest in Europe. Complementary measurements of the particle number size distributions (PNSD) have been conducted using a Differential Mobility Particle Sizer (DMPS) over certain periods and in different environments, in collaboration with Stockholm University. The dynamics observed in the urban PNSD is subject to continued analysis efforts [2].

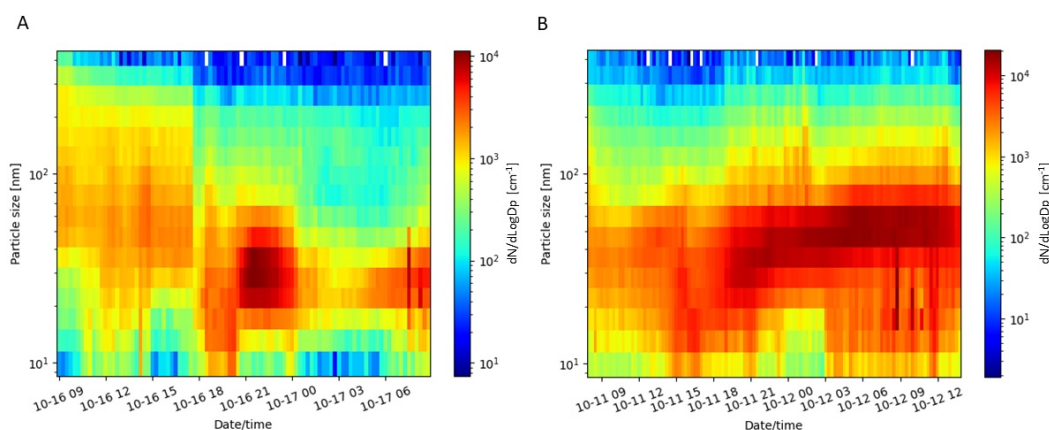


**Figure:** Scavenging (A) and particle growth (B) events in the urban background of Stockholm, Sweden.

In the present work, we focus on the impact of different meteorological parameters from co-located measurements, particularly precipitation, on the PNSD in the urban background in Stockholm, Sweden to better understand its dynamics. These results will help to disentangle factors impacting the PNSD variability.

[1] World Health Organisation (WHO), Air Quality Guidelines 2021

[2] P. Krecl, C. Johansson, M. Norman, S. Silvergren, L. Burman, E. M. Mollinedo, A. Créso Targino; Environmental Pollution 2024, 347, 123734

**An equation describing the wavelength-dependence of brown-carbon light absorption at all wavelengths**

J. C. Corbin<sup>1</sup>, T. A. Sipkens<sup>1\*</sup>

<sup>1</sup>Aerosol and Gas Metrology, National Research Council Canada, Ottawa, Canada

Natural carbonaceous particles from combustion can possess a range of light-absorbing properties, ranging from black soot to brown organics (the “brown-black continuum”). This light absorption is often described in terms of the absorption Angstrom exponent (AAE) power law: the negative slope of a log-log plot of light absorption versus wavelength. Black carbon has a fixed AAE of  $\approx 1.0$  at all wavelengths. However, different values of AAE for brown carbon are observed at different wavelengths (Moosmuller et al., 2011). This wavelength-dependent AAE is predicted by the Tauc model (Sun et al., 2007), which employs two theoretical parameters first derived for semiconductor materials. Here, we reformulate this Tauc model using easily measured aerosol properties: mass-specific light absorption (MAC) and AAE. An equation is provided to extrapolate the MAC and AAE at any arbitrary wavelength, given these properties at a reference wavelength in the visible. Notably, using the black-carbon MAC and AAE as reference accurately describes the available literature data, including soot, pyrolyzed carbon, char, and biomass-burning tarballs. Future work might apply this framework to quantify the spectrally integrated light absorption of brown carbon from unknown atmospheric samples.

Moosmüller, H; Chakrabarty, R. K., Ehlers, K. M., Arnott, W. P. Absorption Angstrom coefficient, brown carbon, and aerosols: basic concepts, bulk matter, and spherical particles. *Atmos. Chem. Phys.*, 11, 1217-1225, 2011.

Sun H., Biedermann L., Bond T.C, Color of brown carbon: A model for ultraviolet and visible light absorption by organic carbon aerosol, *Geophys. Chem. Lett.* 34(L17813), 2007.